Atomic Layer Deposited TiO_2 on a Foam-Formed Cellulose Fibre Network – Effect on Hydrophobicity and Physical Properties

Laura Keskiväli,[a] Tiinamari Seppänen,[b,*] Paavo Porri,[c] Elina Pääkkönen,[b] and Jukka A. Ketoja [a]

Climate change and plastic pollution challenge us to develop alternatives for fossil-based plastics, and cellulose-based materials are excellent candidates for this. Foam forming technology for cellulose fibre products increases process efficiency, widens the raw materials base, and enables low-density structures from fibres. Low-density cellulose-based materials can be used, for example, for packaging, insulation, and construction materials. However, to achieve optimal performance, the resistance against moisture and mechanical compression ought to be enhanced. In this research, the effect of atomic layer deposited (ALD) titanium dioxide on four foam-formed cellulose-based structures was studied. The hydrophobicity of these materials was analyzed with water contact angle measurements. Moisture content and mechanical properties were tested at high humidity (50% RH and 90% RH) by analyzing moisture uptake and compression strength. Furthermore, the morphology and microstructures were evaluated with scanning and transmission electron microscopy (SEM and TEM). ALD treatment changed the hydrophilic materials to hydrophobic with 5 cycles of TiO_2 for all four substrates. The effect on moisture content was milder but was observed strongest with unrefined and partly refined samples at 50% RH. A clear trend between moisture content and mechanical strength was detected since the compression strength increased with decreasing moisture content.

DOI: 10.15376/biores.18.4.7923-7942

Keywords: Foam forming; Cellulose; Fibre network; Atomic layer deposition; Titanium dioxide; Hydrophobicity; Moisture content; Compression strength

*Contact information: a: VTT Technical Research Centre of Finland, P.O. Box 1000, 02044 VTT, Espoo, Finland; b: VTT Technical Research Centre of Finland, P.O. Box 1603, 40101 Jyväskylä, Finland; c: University of Helsinki, Department of Chemistry, P.O. Box 55, FI-00014, Helsinki, Finland; * Corresponding author: tiinamari.seppanen@vtt.fi*

INTRODUCTION

Plastic is a versatile material that is used widely in packaging applications. Plastic consumption is expected to double over the next two decades. Approximately 10% of plastic packaging is recycled (The Ellen MacArthur Foundation 2017); most plastic ends up being incinerated, in landfills, or as pollution. Therefore, alternatives for fossil-based plastics are needed, and materials based on natural fibres, such as cellulosic substrates, are excellent candidates. One noteworthy technique for engineering cellulose substrates is foam forming (Hjelt *et al*. 2022), in which bubbly foam is used as a suspending medium for fibre suspension that enables high air content contained by bubbles. Foam forming

enables the making of a variety of fibre products, which can be used for example in packaging materials, nonwoven fabrics, microelectronics, insulation, construction materials, and biomaterials. The resource and energy-saving technique will promote new uses that include accurate layers, complex shapes, and tailored microstructures (Al-Qararah *et al*. 2015; Härkäsalmi *et al*. 2017; Hjelt *et al*. 2022).

However, to be able to utilize these materials in various applications effectively, researchers need to meet material property requirements for different end-use applications. For example, in packaging or thermal insulation, the materials should stand mechanical stress and recover also in changing climate conditions. Hydrophilic fibres need to be transformed into hydrophobic form to protect their mechanical properties, which otherwise would tend to deteriorate with increasing relative humidity. There are many kinds of surface modification techniques, such as acid oxidation, alkali modification, esterification, and plasma modification, to alter the functional and mechanical properties of fibre materials. However, most of these frequently used techniques are wet chemistry modifications, which have drawbacks including solvent exchange processes and complex disposal of waste solvents. As a way to avoid the burden of these wet chemistry drawbacks, one suitable and flexible technique for fibre modification purpose is atomic layer deposition, ALD. As the foam forming technology was previously described as a "technique producing accurate material layers and complex three-dimensional forms", correspondingly atomic layer deposition can be described as a surface-controlled layer-by-layer process based on self-limiting gas-solid reactions between volatile precursors and reactive sites at the substrate, forming pinhole-free, uniform, and conformal thin films (Leskelä and Ritala 2002; Puurunen 2005; George 2010). One of the most advantageous aspects of ALD is its ability to create conformal films and coatings across a large area with complex roughness and topography. This makes the ALD technique an excellent candidate for modifying foam-formed cellulose surface and physical properties and possibly enhancing water resistance and mechanical properties.

Due to the variable surface structure of fibres and polymers, ALD has been studied as a technique to modify, encapsulate, and coat fibres and textiles to add new multifunctional features (Jur *et al*. 2010; Choi *et al*. 2012; Gui *et al*. 2013; Azpitarte *et al*. 2017). Many research groups have been studying the fundamental aspects of ALD modification of fibre materials and the novel functionalities enabled by ALD (Peng *et al*. 2007; Hirvikorpi *et al*. 2011; Gong and Parsons 2012a; Keskiväli *et al*. 2021). ALD growth on polymer fibres is often non-linear, especially in the beginning of the deposition process and at low temperatures. When coating fibres, it is clear that the coating structure depends strongly on the fibre composition (Puurunen 2005; Chang *et al*. 2008; Lee *et al*. 2009; Zhang *et al*. 2009; Spagnola *et al*. 2010). During the nucleation period, precursors adsorb onto the surface and may absorb into the near-surface regions (Wilson *et al*. 2005; Spagnola *et al*. 2010; Gong and Parsons 2012b; Obuchovsky *et al*. 2016). During the first deposition cycles, metal oxides tend to nucleate and form clusters (Grigoras *et al*. 2008; Vähä-Nissi *et al*. 2012). The different polar groups likely form the basis for nucleation and initial growth, as demonstrated with self-assembled monolayers (Xu and Musgrave 2004). During the first deposition cycles, changes in the surface energy of the base material are related to surface roughness, nucleation effects, and unreactive adsorption sites (Lee *et al*. 2012a; Vähä-Nissi *et al*. 2014). Prolonged exposure to the process conditions or surface pre-modifications negatively affect the film growth, uniformity, and barrier properties (Hirvikorpi *et al*. 2010, 2011).

Cellulose is the most abundant polysaccharide, composed of D-glucose units linked with β-1,4-bonds. In its native form, cellulose has a hydrophilic nature due to the hydroxyl functionalities on the surface. Many research groups have been studying the effect of ALD modification on the hydrophilicity/hydrophobicity of the various kind of cellulose substrates (Kemell *et al*. 2005; Lee *et al*. 2012b; Gregorczyk *et al*. 2015; Mirvakili *et al*. 2016; Short *et al*. 2019; Gregory *et al*. 2020; Li *et al*. 2020; Wooding *et al*. 2020). Gregory *et al*. (2020) tested the effect of single cycle ALD on bulk wood lumber. They tested aluminum oxide (Al_2O_3), zinc oxide (ZnO), and titanium oxide (TiO_2) depositions against mold growth, moisture content, and thermal conductivity. In their study, they conclude that while all ALD chemistries are found to make the wood's surface hydrophobic, wood modified with TiO_2 ($TiCl_4$ + H_2O) shows the greatest bulk water repellency upon full immersion in water. Furthermore, they suggest the superiority of TiO_2 is resulting from the reaction-rate-limited processing kinetics of $TiCl_4$, which enables deeper diffusion of the precursors into the wood's fibrous structure (Elam *et al*. 2003; Gregory *et al*. 2020). The main finding of Wooding and his group was the necessity of adsorbed adventitious carbon (Wooding *et al*. 2020). The same finding has been made by other research groups as well (Hyde *et al*. 2010; Jur *et al*. 2010; Lee *et al*. 2012b; Li *et al*. 2020). ALD coating consists of oxygen-containing functional groups, attracting the adventitious carbon molecules. This enables the formation of hydrocarbon surface, leading to hydrophobicity (Wooding *et al*. 2020). The more specific composition and structure of these adventitious carbon additives are still unclear, but for example, $C_5H_{12}N^+$, $C_8H_5O_3^+$, CH_3^+ and $SiC_3H_9^+$ species have been reported (Mangolini *et al*. 2014). In their study, a few cycle ALD modifications (2-cycles) combined with an additional post-deposition heating step are found to make the cellulose behave in a more hydrophobic manner.

Mirvakili *et al*. (2016) studied refined and unrefined kraft cellulose pulp without any hydrophobic binders, chemical modifiers, or additives. Fibres were modified with 10, 25, and 45 nm Al_2O_3 PE-ALD. In addition to the refinement technique, the fibre size and surface roughness had the largest effect on water vapour transmission rate (WVTR) and air permeability. They concluded that the smaller the fibre is, the lower the roughness and increased hydrophobicity are. Moreover, a thicker ALD coating led to a lower surface roughness and to a reduced change in hydrophobicity (Mirvakili *et al*. 2016). The exact nature of thin film growth on a porous non-woven fibre surface and its effects on the physical properties is still a relatively novel field of research. Thus, the balancing act between moisture resistance and the strength of the material requires careful research. Often, a relatively thick oxide coating may effectively protect the cellulose from moisture and environmental threats, but it can also reduce mechanical flexibility. For this reason, using only a few cycles (1 to 10) is the best option to achieve hydrophobicity and maintain mechanical strength.

In this research, the effect of atomic layer deposition of titanium oxide on porous foam-formed cellulose fibre structures in high humidity was studied. Fibre structures after ALD TiO_2 deposition were characterized with spectroscopic methods and changes in physical properties such as compression strength and moisture content of fibres were measured. Based on the previous studies in the field, (Kemell *et al*. 2005; Gregorczyk *et al*. 2015; Mirvakili *et al*. 2016; Gregory *et al*. 2020; Li *et al*. 2020; Wooding *et al*. 2020), it was decided to study the effect of TiO_2 coating instead of Al_2O_3 or ZnO on foam-formed cellulose to reduce the water vapour transmission, enhance hydrophobicity and improve compression strength.

Although bare TiO_2 is hygroscopic, the process was expected to form a hydrophobic surface with adsorbed adventitious carbon when deposited onto a cellulosic surface using only a few ALD cycles. There have been few studies on the effect of ALD modification on barrier properties of cellulose without any additives or chemical modifiers (Mirvakili *et al*. 2016; Gregory *et al*. 2020). Furthermore, to the knowledge of the authors, this is the first time when the results of ALD modification on foam-formed cellulose is published.

EXPERIMENTAL

Foam-formed Materials

The cellulose-based substrate materials were prepared by the foam forming technique, as described elsewhere (Hjelt *et al*. 2022). The target density and the thickness of the samples were 60 kg/m^3 and 20 mm. The pulp and the surfactant, Simulsol SL10, with a dosage of 1.2 g/L, were placed in a vessel and the fibre foam was generated using a laboratory mixer (Netzsch, Hedensted, Denmark). The target pulp consistency (*i.e.*, mass fraction of the solid material in the suspension) before foam generation was 2.5%. The foam generation time was 5 to 10 min, with a rotational speed of 3800 to 5400 rpm, depending on the fibre mixture. The air content of the wet foams ranged from 54 to 65%. The fibre foam was poured into a hand sheet mould and was left to drain for 20 min in ambient conditions before drying in the oven at 70 °C. To adjust the samples' thickness and density, the dried sheets were re-wetted to reach a solids content of 50% and compressed between metal plates with spacers. This operation required drying the samples again at 70 °C in the oven. An example of the foam-formed pulp samples is shown in Fig. 1 a. Four different sample sets with varying raw pulp materials were prepared (Tables 1 and 2).

Table 1. Raw Pulp Materials Used in the Study

Abbreviation	Raw Pulp Material	Type	Producer
BSKP	Unrefined bleached softwood kraft pulp	SR13, unrefined	Metsä Fibre, Äänekoski Mill, Finland
BSKP SR90	Refined bleached softwood kraft pulp	SR90, refined by Voith laboratory refiner LR1 in KCL, Espoo, Finland	Metsä Fibre, Äänekoski Mill, Finland
CTMP	Spruce chemi-thermomechanical pulp, bleached ISO-75%	CSF600	Rottneros, Rottneros Mill, Sweden

Table 2. Sample Sets and Fibre Combinations for Foam-formed Samples

Sample Set Number	Combinations for Foam-Formed Samples
1	100% BSKP
2	75% BSKP + 25% BSKP SR90
3	50% BSKP + 50% BSKP SR90
4	100% CTMP

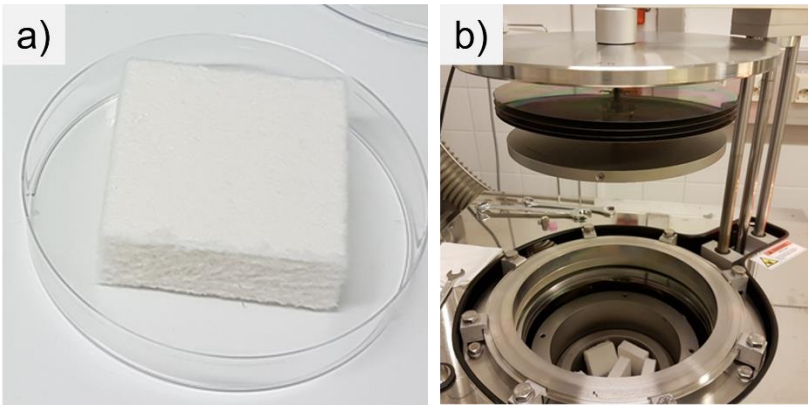

Fig. 1. a) Dried foam-formed softwood kraft pulp sample. b) Foam-formed samples in the Picosun R-200 reactor chamber

ALD TiO_2 Process

ALD modifications were done using an ALD Picosun R-200 tool in single wafer mode (Fig. 1 b). N_2 (>99.999%) from LNG (liquid nitrogen gas) was used as the carrier gas. Two-step processes were constructed from titanium tetrachloride ($TiCl_4$, 99%, Strem Chemicals) as a metal precursor and deionized water (Fig. 2). The ALD process is a cyclic deposition method with self-limiting reactions between the excess amount of gas phase precursors and substrate surface.

Figure 2 presents a schematic illustration of an atomic layer deposition cycle for TiO_2. In the first step, titanium tetrachloride ($TiCl_4$) is pulsed to the surface and during a gas–solid reaction, O-Ti(Cl) and O-$Ti(Cl)_2$ structures are formed on the surface, releasing HCl as a by-product. During the water pulse, hydroxyl structures are formed on the surface and again HCl is released as a by-product. After each precursor pulse, any excess precursors and HCl are removed by inert purging. Titanium oxide coatings were deposited on foam-formed cellulosic substrates and on reference silicon wafers (Si (100), Siltronic Corp.). Both $TiCl_4$ and H_2O precursors were stored in a metallic container and evaporated at room temperature. The deposition temperature was kept constant at 150 °C. Samples were kept at reaction conditions for 4 h before the deposition to ensure the absence of adsorbed water on the fibres.

Several pulsing and purging times were tested, and the average process was 1.0/60/1.0/60 s ($TiCl_4$/purge/H_2O/purge). When stop-flow mode was used, the precursor gases were held in the reaction chamber for 10, 15 or 30 s before purging with inert gas, ensuring adequate precursor diffusion time. The number of deposited cycles were 5 and 15. Also, one additional 100 cycles test run for sample set 1 was carried out. In addition to the totally unmodified reference samples, the so-called ALD reference for unraveling the harsh effects of ALD reactor conditions (150 °C, 6 to 7 hPa) was produced by keeping the fibre material in the ALD reaction chamber for 4 h without deposition.

The film thickness from reference Si wafers was analyzed by ex-situ ellipsometry (Sentech SE400adv). Measurements of the lowest cycle count films (5 and 15 cycles) were inconsistent due to the island-like growth and altogether difficult to perform. Measuring the thicker films indicated a GPC (growth per cycle) approximately of 0.6 Å per cycle, in agreement with the literature (Ritala *et al*. 1993; Sammelselg *et al*. 1998; Aarik *et al*. 2000).

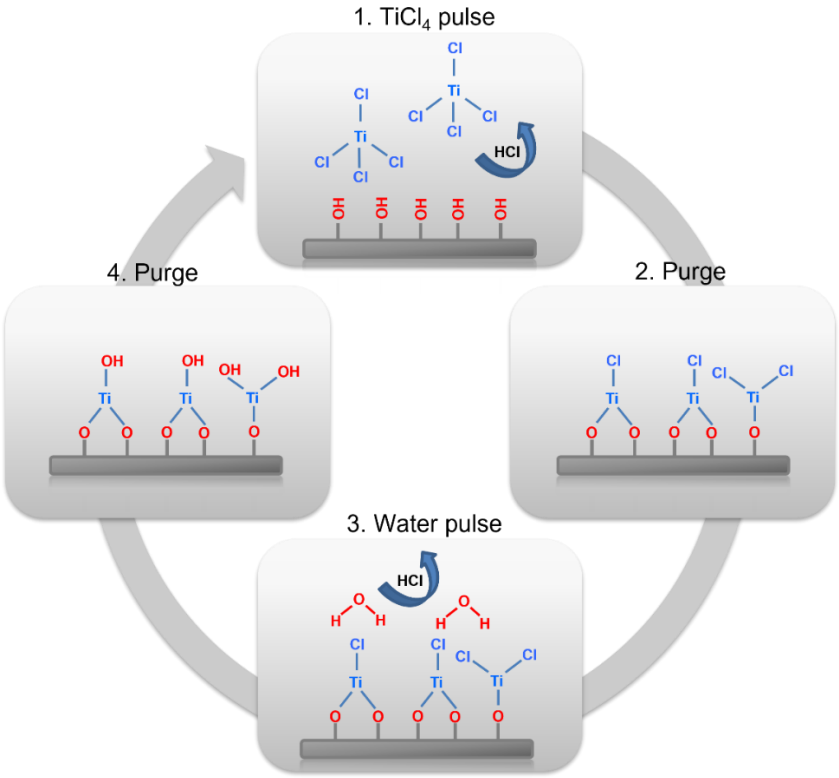

Fig. 2. Atomic layer deposition cycle of $TiCl_4$ + H_2O process. The surface reactions are expected to take place both at the surface of a foam-formed sample as well as inside the porous sample at fibre surfaces.

Characterization and Mechanical Test Methods

The effect of ALD process conditions on a fibre network

Selected samples were exposed to the ALD process conditions without the actual TiO_2 deposition, which resulted in drying of the samples at an elevated temperature and in low pressure. The resulting changes in fibre material properties were analyzed in terms of the measured moisture content and compression tests (see below) in different environments. The equilibration was done at room temperature and at a constant 50% RH (relative humidity) for 24 h before weighing and mechanical testing. After balancing at 50% RH, the samples were balanced at 90% RH for the same characterization.

Scanning electron microscopy (SEM)

Scanning electron microscopy (SEM) was used to inspect a fibre surface. The unmodified sample was compared to a sample with 100 ALD cycles to observe any evident changes in the surface morphology. The sample with 100 cycles was used instead of 5 cycles due to the island-like growth and small amount of material deposited during the first 5 cycles with the growth of 0.6 Å/cycle. Imaging was done with Zeiss Merlin Gemini field emission SEM using the in-lens detector.

Transmission electron microscopy (TEM)

Transmission electron microscopy (TEM) was used to evaluate the possible metal oxide infiltration into the fibres and the homogeneity of ALD film growth throughout the relatively thick fibre networks. Sample preparation and imaging were conducted at the

Electron Microscopy Unit (EMBI) at the University of Helsinki. Imaging was performed using a Jeol JEM-1400 microscope with an accelerating voltage of 120 kV. Magnifications used were from 1200X to 100 000X. Samples were taken from each material sample's top fibre layer and from inside the blocks. The fibre samples were then cast in epoxy, and after curing cut with an ultramicrotome (Leica EM Ultracut UC6i) to 60 nm thickness.

Water contact angle analysis

To verify the ALD growth and to see some immediate effects of the TiO_2 coating on the fibres, contact angle measurements were performed with a Biolin Scientific Attension Theta optical tensiometer. Deionized water was used to determine the hydrophobicity of the foam-formed sample surface. Samples were stabilized for 24 h (21 °C, RH 50%) before the measurements. Droplet size was varied between 5 and 10 μL. The camera was set to a maximum frame rate (360 fps). The measurement lasted for a maximum of two min.

Moisture content of equilibrated samples

The MC (moisture content) of the samples was measured at 50% and 90% RH. First, the samples were balanced overnight in an air-conditioned laboratory room (23 °C, RH 50%) and the mass was measured. Next, the samples were placed into the climate chamber having RH of 90% for 24 h. Finally, samples were dried in an oven at 105 °C.

Compression strength

Compression strength at 50% and 90% RH was measured for the ALD-modified samples both with and without the TiO_2 deposition. The sample size was 50 mm × 50 mm × 20 mm, cut with a band saw. Cyclic compression tests were run with a Lloyd LR10K universal tester (Lloyd Instruments Ltd, Bognor Regis, West Sussex, UK) with a 1 kN sensor. The strength was obtained as a stress value at 10% and 50% compression levels. The test speed for the 20 mm sample was 2 mm/min for the 10% compression and 20 mm/min for the subsequent 50% compression. A total of 3 to 4 parallel samples were tested per trial point.

RESULTS AND DISCUSSION

The Effect of ALD Process Conditions without TiO_2 Deposition

BSKP samples (sets 1-3)

The elevated temperature of 150 °C during the ALD process condition exposure led to a mass loss of approximately 1 to 2% for the BSKP samples, measured at 50% RH. Most probably this was due to the decreased equilibrium moisture content (MC) because remarkable degradation and evaporation of the polymeric fibre materials (lignin and hemicelluloses) was not expected to happen at this temperature. This was indicated also by the fact that the obtained samples without TiO_2 deposition (called ALD references) did not show any colour change. The compression strength and MC of these samples can be seen in Fig. 2. The comparison with non-modified samples shows quite strong effects coming from the ALD environment alone without any applied surface layers. In sets 1 (100% BSKP) and 3 (50% BSKP + 50% BSKP SR90), the moisture content decreased, and the compression strength increased compared to the non-modified reference. The decrease in

MC and increase in strength were higher at 50% RH, but a similar trend can be seen also at 90% RH.

Sample set 2 (75% BSKP + 25% BSKP SR90) behaved differently compared to sets 1 and 3. There was only a small decrease in MC at 50% RH, and the compression strength increased only slightly after exposure to the ALD process conditions. At 90% RH, there was no change in MC and the compression strength even decreased.

The change in moisture content and compression strength of the BSKP samples could be due to fibre hornification and thermally induced softening of the hemicellulose. In hornification, the internal fibre volume shrinks as a result of drying, and when the fibre network is rewetted, the fibres do not swell to the same extent as before the drying. This can be seen from the decrease in moisture uptake in sample sets 1 to 3, especially at 50% RH. Hornification affects the elasticity of the fibres when the lignin content of the pulp is very low. As a result, the drying makes BSKP fibres stiffer. The most of the hornification occurred probably already during drying at the pulp mill, but due to the harsh conditions during the ALD-modification, some further hornification of the fibres in addition to the conversion of the hemicellulose probably took place.

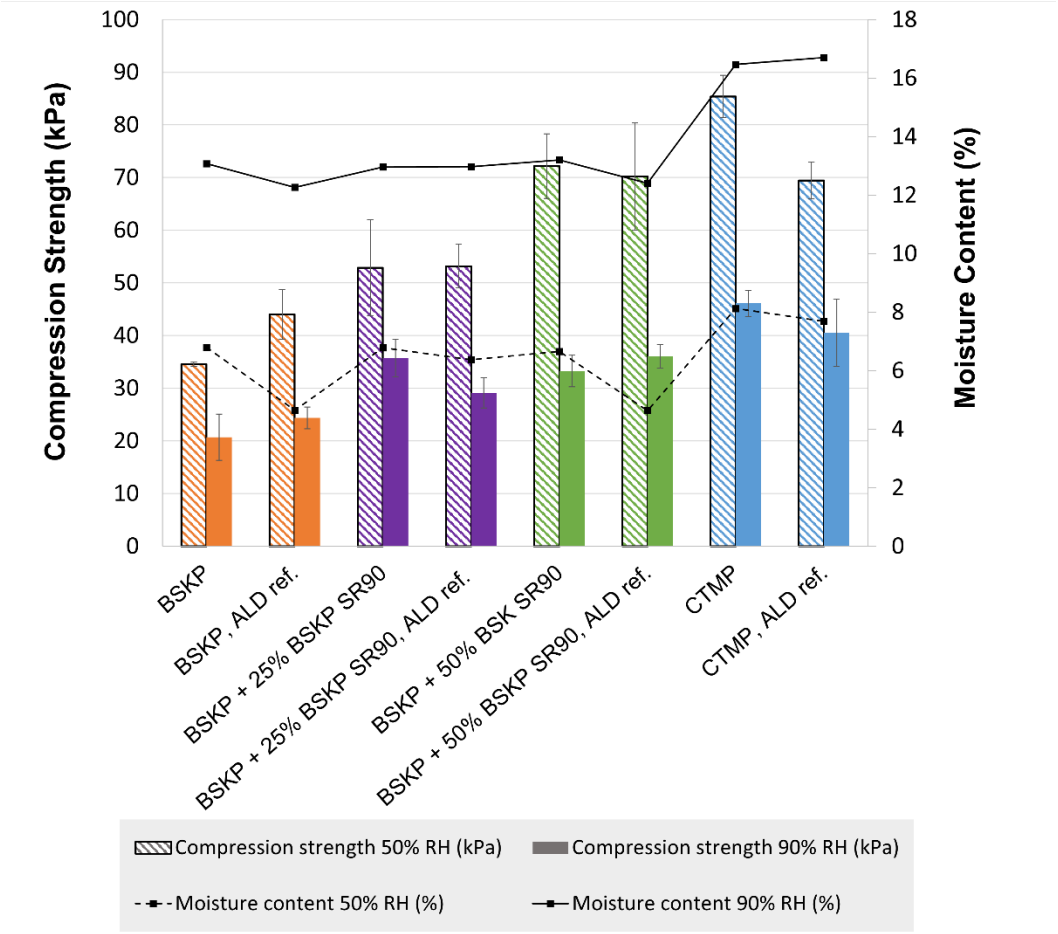

Fig. 3. The compression strength and moisture content of the samples at 50% and 90% RH after exposure to ALD reaction conditions without deposition. Set 1) BSKP, Set 2) 75% BSKP+ 25% BKSP SR90, Set 3) 50% BSKP + 50 % BSKP SR90, Set 4) CTMP.

CTMP samples (set 4)

In visual inspection, the ALD references showed a slight change of colour from light yellow to darker yellow (samples were initially light yellow, due to a small amount of lignin). Figure 3 shows the compression strength and moisture content of the samples. The higher MC level compared to BSKP fibres is caused by the high fines content of CTMP and the high moisture uptake capacity of the fines. The fines are known to contribute significantly to bonding of the CTMP fibres, and therefore any drying-induced changes in the morphology of fines can affect the material strength. Compared to the reference, the ALD reference had slightly lower MC at 50% RH and higher MC at 90% RH but these changes in MC were minor. Thus, the observed strength drop of the ALD reference was probably caused by the reduced bonding ability of the fines. The relative decrease in strength caused by ALD environmental exposure was clearly smaller at 90% RH probably because of the difference in the dominant water fraction.

Scanning Electron Microscopy

Fibre surface structure was studied before and after the TiO_2 deposition. A reference BSKP sample was compared to a BSKP sample with 100 cycles of TiO_2 deposition, Figs. 4 a, b and Figs. 4 c, d, respectively. Visible cracking of the fibre fine structure was observed on both samples, but the sample with ALD thin film exhibited slightly less pronounced cracking, since the ALD film smoothens the fibre surface.

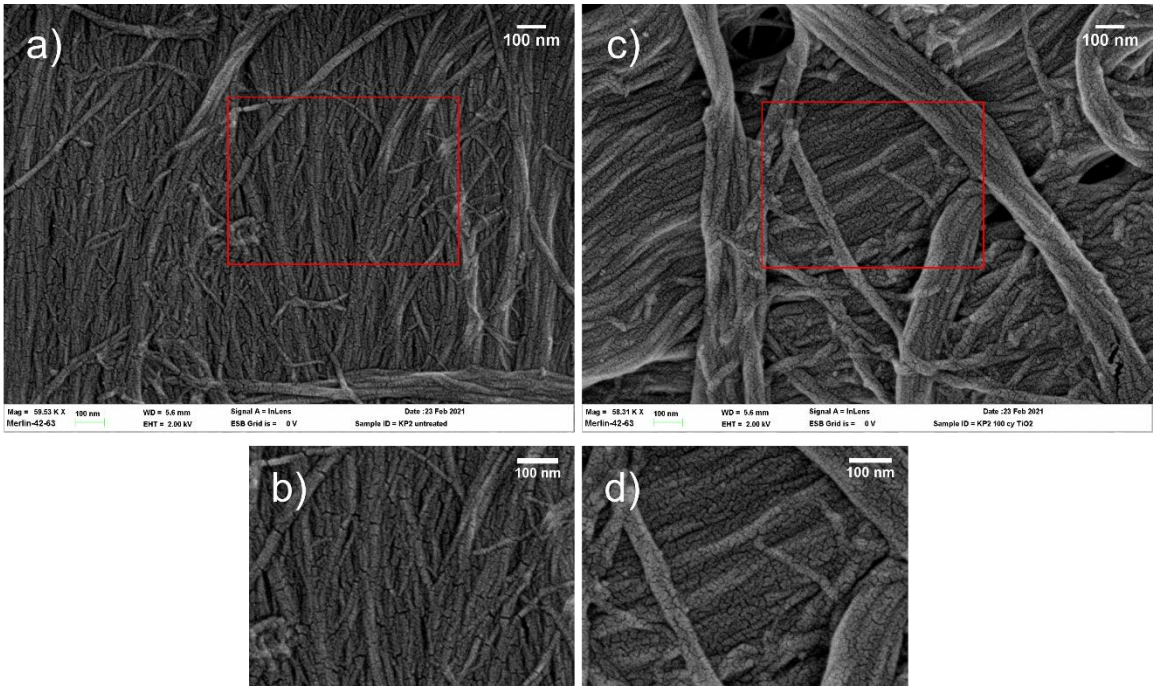

Fig. 4. a) and b) SEM image of BSKP fibre without ALD modification, c) and d) SEM image of BSKP fibre with 100 ALD cycles of TiO_2

Transmission Electron Microscopy

The relatively high temperature and stop-flow process parameters were thought to help precursors infiltrate into the fibres. However, it seems that the oxide growth did not extend past the top surface layer of the fibre. TEM imaging (Fig. 5 a) shows a sharp

interface between the fibre and the metal oxide layer, with no visible infiltration into the fibre. This suggests the presence of abundant hydroxyl groups on the fibre surface reacting with ALD precursors, with no apparent metal oxide nucleation in the sub-surface region. This TEM image and results are in line with the previous study of Jur *et al*. (2010), although with different precursors ($TiCl_4$ vs. TMA) and higher temperature.

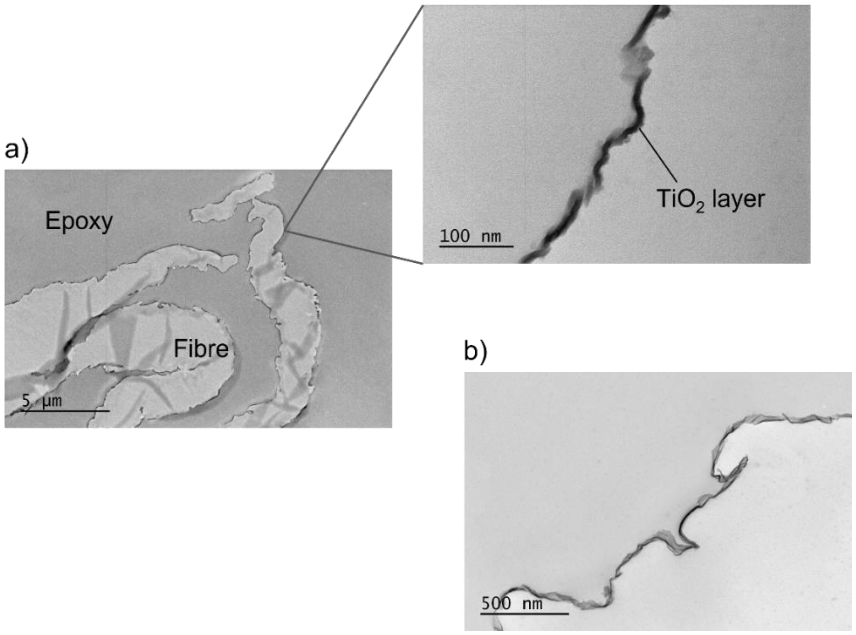

Fig. 5. a) TEM images of the BSKP sample with 100 ALD cycles. The sample was taken from the surface of the foam-formed block. b) TEM image of the sample with 100 ALD cycles. The sample was taken from inside the foam-formed fibre block with thickness of 2 cm.

Furthermore, samples from the surface of the fibre block were compared to samples taken from inside the fibre block (block thickness 2 cm), with no visible difference between the layer thickness or uniformity (Fig. 5 b). In other words, the TiO_2 material was deposited both on the surface of the sample block as well as at the fibre surfaces inside the block. Hence it can be said that chosen process parameters were suitable for covering a rather high surface area of complex cellulose network with a thin film.

The ALD set up and process parameters were similar to the previously published vapour phase infiltration study, where ALD precursors were successfully infiltrated into the cellulose fibres (Gregorczyk *et al*. 2015). Having this in mind, it was slightly surprising that no verified infiltration happened in the present research, since only the pronounced interface between the ALD layer and fibre surface was detected by TEM imaging. However, we cannot completely exclude the possibility of the existence of nano-scale nucleation layers within the microfibril bundle structures not visible in TEM imaging due to the used resolution. Further elucidation of the precursor infiltration dynamics was deemed outside the scope of this study.

Water Contact Angle

Water contact angles were measured to discover the immediate effect of the ALD modification on the hydrophobicity of the fibres. With a low number of ALD cycles, island-like clusters were formed on the cellulose fibres. Hydrophobicity is likely to be caused by carbon species adsorbing from the atmosphere (adventitious carbon) onto the

ALD oxide clusters. This enables the formation of a hydrocarbon surface, leading to hydrophobicity. This phenomenon is discussed in the introduction section. TiO_2 is intrinsically hydrophilic, so adding more ALD cycles leads to the coalescence of the clusters and thin film formation. This should transform the coated fibre surface back to hydrophilic but could still enhance the mechanical properties. Furthermore, the relatively reduced roughness and changed surface energy can cause a decrease in hydrophobicity. As might be expected based on the literature and these above-mentioned aspects, the water contact angles (WCA) were highest with 5 ALD cycles in our studies. When more cycles were added, regardless of the fibre material, the WCA decreased with an increasing number of cycles. The WCA of the unmodified fibre references and ALD condition references were not possible to measure since the water was absorbed immediately. Therefore, it can be said that the references were completely hydrophilic, and exposing the material to ALD process conditions did not induce hydrophobicity.

For example, when studying the effect of the number of ALD cycles on the sample set 3 substrate material (50% BSKP + 50% BSKP SR90), a water droplet on an ALD reference sample absorbed immediately, as in the case of all fibre substrates without an ALD thin film. With 5 TiO_2 deposition cycles, good hydrophobicity was reached so that a droplet stayed on the fibre surface over 110 s, without a sign of absorption (Fig. 6 a). When the cycle amount was increased to 15, the contact angle was first the same as with 5 cycles but started to decrease quite rapidly already after two seconds. These results are in line with the literature (Lee *et al*. 2012b; Short *et al*. 2019), since for example Gregory *et al*. (2020) concluded that one cycle was enough to induce hydrophobicity on the wood lumber surface. Thus, it can be concluded that with 5 cycles of TiO_2, the carbon species adsorptive island-like clusters are grown, and with 15 cycles the clusters are starting to coalesce, and a hydrophilic thin film starts to take form.

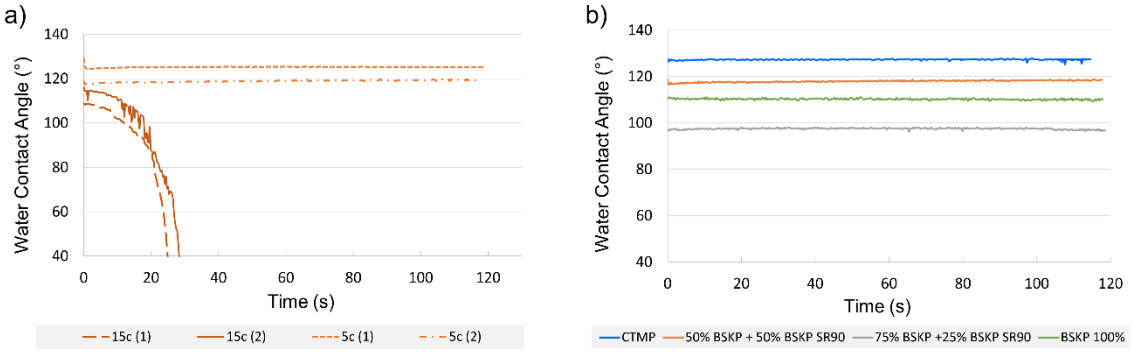

Fig. 6. a) Comparing the water contact angles of 5 (two parallels) and 15 (two parallels) cycles of ALD TiO_2 on 50% BSKP + 50% BSKP SR90, sample set 3. b) Water contact angles of all sample sets 1-4 with 5 cycles of ALD TiO_2. Green: BSKP 100% Set 1, grey: 75% BSKP + 25% BSKP SR90 Set 2, orange: 50% BSKP + 50% BSKP SR90 Set 3, blue: CTMP Set 4.

Comparison between the regular ALD process cycle and the stop-flow (SF) samples indicates that stop-flow enhanced the fibre hydrophobicity. For example, with the fibre material set 3, the initial WCA was around 100° with both methods, but when deposited without SF, the WCA started to decrease quite rapidly after 10 seconds. This can be due to the reaction-limited process nature of $TiCl_4$, as discussed previously by Gregory *et al*. (2020). They mention in their study, that because of the process nature, $TiCl_4$ precursor reaches well to the ends of the pore structures, leading easily to chemical vapour deposition (CVD) type of growth if sufficient purge times are not used. In the case of stop-flow, the

reactants have more time to diffuse out of the pores compared to the normal ALD process with continuous carrier gas flow, with a faster pulsing sequence.

Finally, in the case of water contact angles, the WCA, *i.e.*, hydrophobicity of the ALD-modified fibres increased with an increasing percentage of refined fibres, with an exception for the sample set 1 of 100% BSKP, which was placed between sets 2 and 3 (Fig. 6 b). As concluded by Mirvakili *et al*. (2016), also in the authors' studies, the fibre mean width and fibril-area were higher in more refined fibres, affecting hydrophobicity. When comparing the different fibre materials (BSKP with altering addition levels of refined pulp and CTMP) for an equal number of ALD cycles (5), it can be observed that the material with the highest fines content, CTMP (set 4), had the highest initial contact angle, and the initial WCA decreased with decreasing proportion of refined fibres for BSKP (Fig. 6 b). An exception was found in the case of sample sets with 75% BSKP + 25% BSKP SR90 and 100% BSKP, since the 100% BSKP sample seemed to be more hydrophobic with higher water contact angle. All the measured contact angles were in the relatively narrow range (from 98 to 127°), and there was some variation between replicate measurements (the most representative measurement in each case was chosen for Fig. 6 b). This variation could account for the exception between sample sets 1 and 3. Another possible explanation is the variation of the fibre composition in a foam-formed material and the variation of the thickness of the deposited material on the fibre block.

There is a question about surfactant used in the foam forming process and its residues (Viitala *et al*. 2020). It is possible that the residues affect the ALD coating formation and properties. Because the hydrophobicity was reached with 5 cycles of TiO_2 in all fibre sample sets, it is likely that there were only slight amounts of nonionic surfactants left in the fibre blocks. The anionic surfactant residues tend to retain the fibre surface hydrophilic, despite the ALD modification and that the ALD growth and coating formation is hindered due to the anionic surfactants. However, it is possible that the slight amount of residual nonionic surfactant used in the present study caused, for example, the exception in Fig. 6 b.

Equilibrium Moisture Content of Samples after the TiO_2 ALD Modification

The weight of the samples compressed at 90% RH was measured both at 50% RH and at 90% RH. After drying the samples in the oven to bone dry, their moisture contents (MC) were determined (Fig. 7).

BSKP samples

At 50% RH, the MC of the ALD-modified samples in sets 1 to 3 were generally quite similar. With 15 cycles, a greater difference (16 to 18%) was seen between sets 1 (100% BSKP) and 2 (75% BSKP + 25% BSKP SR90). At 50% RH, the MC of the ALD reference in set 2 decreased only slightly, and the MC of the ALD-modified samples was at the same level as in sets 1 (100% BSKP) and 3 (50% BSKP + 50% BSKP SR90). In sets 1 and 3, the ALD-modified samples had higher MC than the ALD reference.

A clear exception was the sample of set 1 with 100 cycles, whose MC decreased to a half at 50% RH. This suggests that with 100 cycles the surface of the fibres was completely covered by the TiO_2 film, and the possible diffusion of water vapour into the fibres was very slow at 50% RH. At 90% RH, the thick hygroscopic TiO_2 layer may absorb more moisture and speed up water diffusion to a similar level as with 5 and 15 cycles. When the humidity increased from 50% to 90% RH, the differences in MC between the ALD-modified samples almost disappeared. As mentioned in the study of Mirvakili *et al*.

(2016), for uncoated paper-based materials at higher than 50% RH, the water vapour transmission is expected to increase due to the swelling of fibres (Spence *et al*. 2010; Nair *et al*. 2014; Mirvakili *et al*. 2016). The same happens to our foam-formed cellulose samples (sets 1 to 4) as well. The sample with 100 ALD cycles had still lower MC than the references or other ALD-modified samples. The highly refined fibres (in set 3) increased the MC only slightly.

Although the differences were small, the moisture content of the ALD-modified samples and the ALD references decreased systematically for all sample sets (1 to 3) at both 50% and 90% RH when compared to the unmodified references. This is probably due to the conditions in the ALD chamber causing the hornification of the fibres and to the modified surface structure caused by the deposited TiO_2 material. The combined mechanisms of the island-like growth for a few cycles of TiO_2, adsorbed adventitious carbon, hygroscopicity of a thicker and uniform TiO_2 film, and opening of the fibres again in high humidity are quite complex and would need further research for example with NMR and IR techniques.

CTMP samples

The MC of the CTMP samples was higher than that of the BSKP samples, which is expectable since the fines of the mechanical pulp often contain more moisture than the amount in chemical fibres. At 50% RH, the MCs of the ALD-modified samples were lower compared to the ALD reference. Like in the BSKP samples, the MC of the sample with 15 cycles was lower compared to 5 cycles. At 90% RH, the MC of the CTMP samples were also lower than the MC of the references.

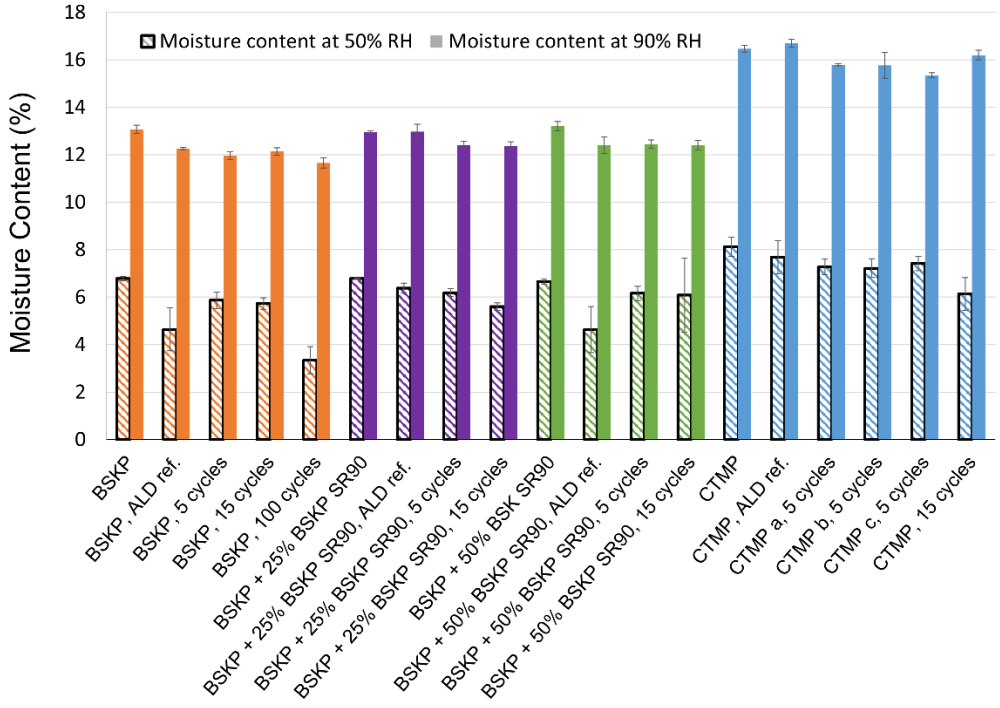

Fig. 7. Moisture content of the samples compressed at 90% RH, first balanced at 50% RH, and then balanced at 90% RH. Set 1) BSKP, Set 2) 75% BSKP + 25% BKSP SR90, Set 3) 50% BSKP + 50 % BSKP SR90, Set 4) CTMP

Interestingly, in this environment the sample with 15 cycles had higher MC than the samples with 5 cycles, as opposed to the results at 50% RH. The prolonged stop-flow time did not affect the MC at 50%, but it seemed to decrease the MC at 90% RH. With prolonged stop-flow time, the purpose was to ensure the proper diffusion and desorption of the $TiCl_4$ and H_2O reagents and prevent non-self-limiting CVD of TiO_2 material further affecting the formation of thicker hydrophilic TiO_2 structure. Apparently, this phenomenon can be observed at substantial humidity of 90% RH.

The water contact angle (WCA) and moisture content results seem to be somewhat contradictory to each other. With 5 cycles of ALD TiO_2, the fibre samples were hydrophobic. When the number of cycles was increased, the surfaces became hydrophilic again. On the other hand, 15 cycles of ALD TiO_2 led to the lowest moisture content (when excluding the case of 100 cycles). Similarly, Mirvakili *et al*. (2016) observed that "although ALD treatment greatly improves the wettability of unrefined hand sheets, it did not affect their WVTR significantly. However, for refined hand sheets the WVTR decreased 97% after Al_2O_3 deposition." (Mirvakili *et al*. 2016). In the present work, differences were observed between sample sets and the amount of refined fibre material in our study as well since there was an increase in MC in highly refined fibres. However, it should be noted that the WVTR and moisture content analysis are two rather different techniques. Yet, both describe moisture barrier properties of a material and in this case the effect of the ALD modification on that property. Finally, too detailed comparison to the literature is difficult, since the coating materials, the number of cycles and substrates vary a great deal, causing an excessive variation in hydrophilic properties in substrates, coatings and in combined influences.

As concluded in the literature, the fibre size and surface properties, depending on the type and extent of refining, can play a crucial role in permeability and absorption of gases. The thickness of the ALD layer has a far less effective role in this, contrary to wettability and water contact angles, where the number of ALD cycles have a strong effect. When the fibre size is decreased due to the refining, the surface area increases, enhancing bonding between the fibres and resulting in denser fibre network with smaller and more uniform pore sizes. This increases the tortuosity in the substrate and thus lowers the permeability (Mirvakili *et al*. 2016; Nair *et al*. 2014). In the present study, the foam-formed cellulose material had high porosity and thus relatively high permeability for water vapour. Therefore, the differences in permeability through the network was not expected to affect the measured equilibrium moisture contents.

Compression Strength

The compression strength was measured at 50% and 90% RH. The compression strength increased with the increasing amount of refined fibres, and the CTMP samples had higher compression strength than the BSKP samples. These general observations due to the different fibre types were as expected. In below, the results of the BSKP samples and CTMP samples are discussed separately. Previously, ALD has been used successfully to improve the strength of polymeric nanofibrous aerogels when the Young's modulus of aerogels increased from 5.54 to 33.27 kPa (Lu *et al*. 2020). There are no references of using ALD with foam-formed cellulose, but the hypothesis for improvement in compression strength proved to be correct for this type of sample as well.

BSKP samples

Figure 8 shows the results of the BSKP samples: Set 1) BSKP, Set 2) 75% BSKP + 25% BKSP SR90, and Set 3) 50% BSKP + 50 % BSKP SR90. The effect of ALD coating on refined fibres was seen more clearly at 50% RH than at 90% RH. The results for some of the trial points had a rather high standard deviation, especially those of the set 3. In set 1, the ALD-modified samples had higher compression strength than the reference at 50% RH. At 90% RH, the strength of the coated samples was similar to that of the ALD reference, and the number of ALD cycles had no effect. The sample with 100 cycles had the highest compression strength among the set 1 at 50% RH. For the set 2, the ALD-modified samples had higher compression strength than the references at 50% RH. The sample with 15 cycles had higher strength than the sample with 5 cycles. For the set 3, the standard deviation was rather high at 50% RH, and there was no clear variation in the measured compression strength values. At 90% RH, the sample with 5 cycles had higher strength than the references, but the samples with 15 cycles were at the same level as the ALD reference.

In summary, it seems that the ALD coating had an effect on compression strength mainly through the equilibrium moisture content at 50% RH. When the moisture content decreased, compression strength increased by approximately 4 to 18%, depending on the sample set for both moisture contents, 50% RH and 90% RH (Fig. 8).

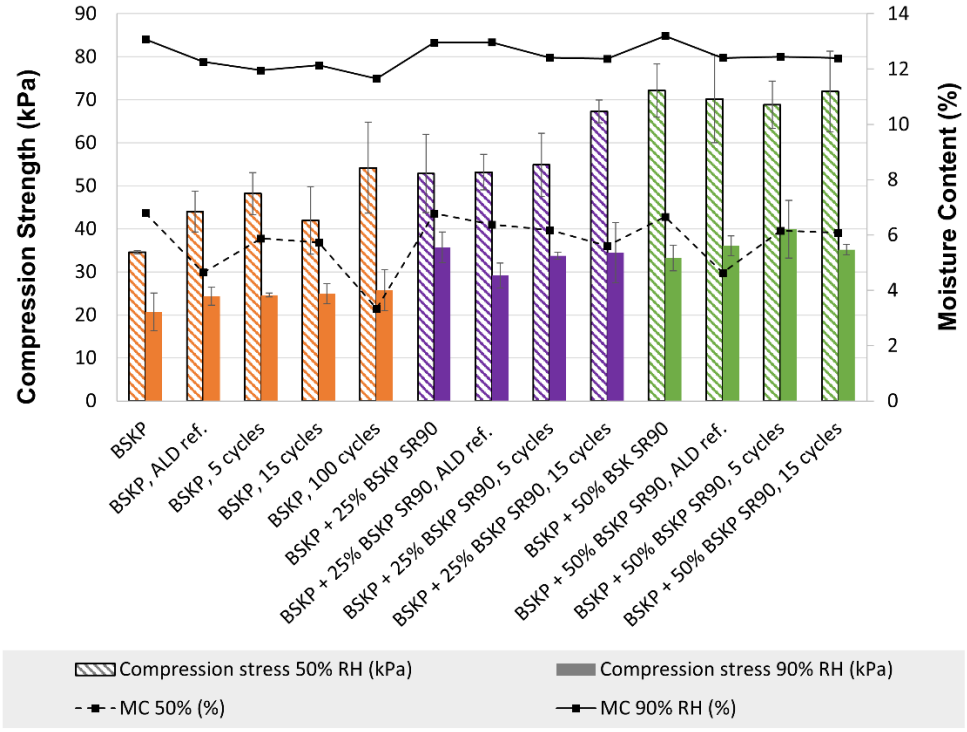

Fig. 8. The compression strength (kPa) and moisture content (%) of the samples. Set 1) BSKP, Set 2)75% BSKP + 25% BKSP SR90, Set 3) 50% BSKP + 50 % BSKP SR90

CTMP samples

The ALD-modified samples had slightly higher compression strength than the references at both humidity levels, as shown in Fig. 9. At 50% RH, the standard deviation of measurements for some of the samples was rather high, but an increase in strength was still seen compared to the ALD reference. At 90% RH, the compression strength was higher

with 15 cycles than with 5 cycles, even though the MC of the sample with 15 cycles was a bit higher.

These results bring insightful aspects for the development work of novel packaging materials, insulation, and construction materials. However, more thorough studies with FTIR, AFM, XPS, and NMR would bring new information of the precursor interactions and coordination during the ALD deposition. In addition, it would be interesting to study other ALD materials, such as Al_2O_3 and ZnO deposited on loose fibre networks, and the effect of post-heat modification of ALD-modified samples on moisture resistivity and compression strength.

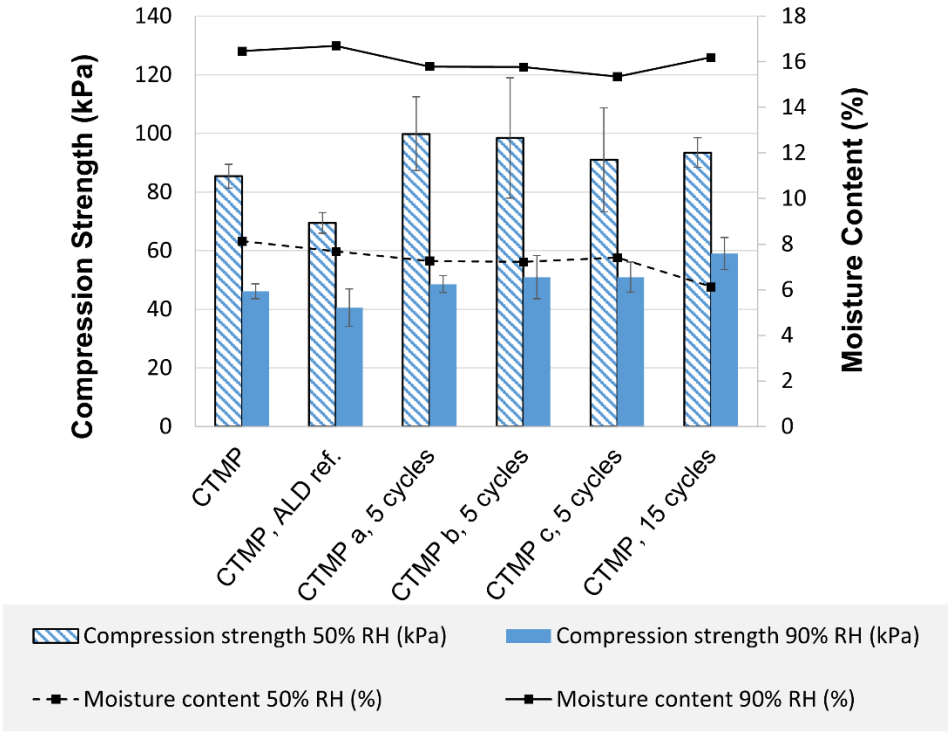

Fig. 9. Compression strength (kPa) and moisture content (%) of the CTMP sample, Set 4. Letters a,b and c refer to the process stop-flow times 10, 15 and 30 s, respectively.

CONCLUSIONS

1. To the knowledge of authors, this was the first time that atomic layer deposited (ALD) TiO_2 has been deposited on a foam-formed cellulose fibre network. The effect of titanium dioxide ALD modifications was studied related to wettability, equilibrium moisture content, and compression strength. The TiO_2 ALD modification affected all the above properties.
2. According to water contact angle measurements, the complete hydrophobicity due to the adsorbed adventitious carbon was reached with all the sample types with 5 cycles of TiO_2 ALD.
3. The effect of ALD modification on equilibrium moisture content of the materials was milder compared to the water contact angles. The strongest effect was noticed at the

50% RH, when the TiO_2 ALD modification decreased the moisture content by 4 to 18%, depending on the sample set. Furthermore, due to the MC decrease, the compression strength increased by 14 to 18%. Overall, TiO_2 ALD modification seemed to have the strongest effect on the fibre samples with unrefined and partly refined kraft pulp fibres.

ACKNOWLEDGMENTS

This research was funded by EU Regional Development Fund, project Piloting Alternatives for Plastics. European Regional Development Fund under Grants A73089 and A73092.

The authors thank Mervi Lindman and the Electron Microscopy Unit of the Institute of Biotechnology, University of Helsinki for providing laboratory facilities.

REFERENCES CITED

Aarik, J., Aidla, A., Mändar, H., and Sammelselg, V. (2000). "Anomalous effect of temperature on atomic layer deposition of titanium dioxide," *J. Cryst. Growth* 220(4), 531-537. DOI: 10.1016/S0022-0248(00)00897-6

Al-Qararah, A. M., Ekman, A., Hjelt, T., Ketoja, J. A., Kiiskinen, H., Koponen, A., and Timonen, J. (2015). "A unique microstructure of the fiber networks deposited from foam-fiber suspensions," *Colloids Surfaces A Physicochem. Eng. Asp.* 482, 544-553. DOI: 10.1016/j.colsurfa.2015.07.010

Azpitarte, I., Zuzuarregui, A., Ablat, H., Ruiz-Rubio, L., López-Ortega, A., Elliott, S. D., and Knez, M. (2017). "Suppressing the thermal and UV sensitivity of kevlar by infiltration and hybridization with ZnO," *Chem. Mater.* 29, 10068-10074. DOI: 10.1021/acs.chemmater.7b03747

Chang, C. Y., Tsai, F. Y., Jhuo, S. J., and Chen, M. J. (2008). "Enhanced OLED performance upon photolithographic patterning by using an atomic-layer-deposited buffer layer," *Org. Electron.* 9(5), 667-672. DOI: 10.1016/j.orgel.2008.04.009

Choi, D. W., Kim, S. J., Lee, J. H., Chung, K. B., and Park, J. S. (2012). "A study of thin film encapsulation on polymer substrate using low temperature hybrid ZnO/Al_2O_3 layers atomic layer deposition," *Curr. Appl. Phys.* 12, 19-23. DOI: 10.1016/j.cap.2012.02.012

Elam, J. W., Routkevitch, D., Mardilovich, P. P., and George, S. M. (2003). "Conformal coating on ultrahigh-aspect-ratio nanopores of anodic alumina by atomic layer deposition," *Chem. Mater.* 15(18), 3507-3517. DOI: 10.1021/cm0303080

George, S. M. (2010). "Atomic layer deposition: An overview," *Chem. Rev.* 110, 111-131. DOI: 10.1021/cr900056b

Gong, B., and Parsons, G. N. (2012a). "Quantitative in situ infrared analysis of reactions between trimethylaluminum and polymers during Al_2O_3 atomic layer deposition," *J. Mater. Chem.* 22(31), 15672-15682. DOI: 10.1039/c2jm32343e

Gong, B., and Parsons, G. N. (2012b). "Quantitative in situ infrared analysis of reactions between trimethylaluminum and polymers during Al_2O_3 atomic layer deposition," *J. Mater. Chem.* 22(31), article 15672. DOI: 10.1039/c2jm32343e

Gregorczyk, K. E., Pickup, D. F., Sanz, M. G., Irakulis, I. A., Rogero, C., and Knez, M. (2015). "Tuning the tensile strength of cellulose through vapor-phase metalation," *Chem. Mater.* 27(1), 181-188. DOI: 10.1021/cm503724c

Gregory, S. A., Mcgettigan, C. P., Mcguinness, E. K., Rodin, D. M., Yee, S. K., and Losego, M. D. (2020). "Single-cycle atomic layer deposition on bulk wood lumber for managing moisture content, mold growth, and thermal conductivity," *Langmuir* 36(7), 1633-1641. DOI: 10.1021/acs.langmuir.9b03273

Grigoras, K., Franssila, S., and Airaksinen, V. M. (2008). "Investigation of sub-nm ALD aluminum oxide films by plasma assisted etch-through," *Thin Solid Films* 516(16), 5551-5556. DOI: 10.1016/j.tsf.2007.07.121

Gui, Z., Zhu, H., Gillette, E., Han, X., Rubloff, G. W., Hu, L., and Lee, S. B. (2013). "Natural cellulose fiber as substrate for supercapacitor," *ACS Nano* 7(7), 6037-6046. DOI: 10.1021/nn401818t

Härkäsalmi, T., Lehmonen, J., Itälä, J., Peralta, C., Siljander, S., and Ketoja, J. A. (2017). "Design-driven integrated development of technical and perceptual qualities in foam-formed cellulose fibre materials," *Cellulose* 24(11), 5053-5068. DOI: 10.1007/s10570-017-1484-6

Hirvikorpi, T., Vähä-Nissi, M., Harlin, A., Marles, J., Miikkulainen, V., and Karppinen, M. (2010). "Effect of corona pre-treatment on the performance of gas barrier layers applied by atomic layer deposition onto polymer-coated paperboard," *Appl. Surf. Sci.* 257(3), 736-740. DOI: 10.1016/j.apsusc.2010.07.051

Hirvikorpi, T., Vähä-Nissi, M., Vartiainen, J., Penttila, P., Nikkola, J., Harlin, A., Serimaa, R., and Karppinen, M. (2011). "Effect of heat-treatment on the performance of gas barrier layers applied by atomic layer deposition onto polymer-coated paperboard," *J. Appl. Polym. Sci.* 122, 2221-2227. DOI: 10.1002/app.

Hjelt, T., Ketoja, J. A., Kiiskinen, H., Koponen, A. I., and Pääkkönen, E. (2022). "Foam forming of fiber products: A review," *J. Dispers. Sci. Technol.* 43(10), 1462-1497. DOI: 10.1080/01932691.2020.1869035

Hyde, G. K., Scarel, G., Spagnola, J. C., Peng, Q., Lee, K., Gong, B., Roberts, K. G., Roth, K. M., Hanson, C. A., Devine, C. K., Stewart, S. M., Hojo, D., Na, J. S., Jur, J. S., and Parsons, G. N. (2010). "Atomic layer deposition and abrupt wetting transitions on nonwoven polypropylene and woven cotton fabrics," *Langmuir* 26(4), 2550-2558. DOI: 10.1021/la902830d

Jur, J. S., Spagnola, J. C., Lee, K., Gong, B., Peng, Q., and Parsons, G. N. (2010). "Temperature-dependent subsurface growth during atomic layer deposition on polypropylene and cellulose fibers," *Langmuir* 26(11), 8239-8244. DOI: 10.1021/la904604z

Kemell, M., Pore, V., Ritala, M., Leskelä, M., and Lindén, M. (2005). "Atomic layer deposition in nanometer-level replication of cellulosic substances and preparation of photocatalytic TiO_2/cellulose composites," *J. Am. Chem. Soc.* 127(41), 14178-14179. DOI: 10.1021/ja0532887

Keskiväli, L., Heikkilä, P., Kenttä, E., Virtanen, T., Rautkoski, H., Pasanen, A., Vähä-nissi, M., and Putkonen, M. (2021). "Comparison of the growth and thermal properties of nonwoven polymers after atomic layer deposition and vapor phase infiltration," *Coatings* 11(9). DOI: 10.3390/coatings11091028

Lee, K., Jur, J. S., Kim, D. H., and Parsons, G. N. (2012a). "Mechanisms for hydrophilic/hydrophobic wetting transitions on cellulose cotton fibers coated using Al_2O_3 atomic layer deposition," *J. Vac. Sci. Technol. A Vacuum, Surfaces, Film.* 30

(1), 01A163-7. DOI: 10.1116/1.3671942

Lee, K., Jur, J. S., Kim, D. H., and Parsons, G. N. (2012b). "Mechanisms for hydrophilic/hydrophobic wetting transitions on cellulose cotton fibers coated using Al_2O_3 atomic layer deposition," *J. Vac. Sci. Technol. A Vacuum, Surfaces, Film* 30(1), 01A163. DOI: 10.1116/1.3671942

Lee, S.-M., Grass, G., Kim, G.-M., Dresbach, C., Zhang, L., Goselea, U., and Knez, M. (2009). "Chemistry and physics of metal oxide nanostructures," *Phys. Chem. Chem. Phys.* 11(19), 3608-3614. DOI: 10.1039/b905768d

Leskelä, M., and Ritala, M. (2002). "Atomic layer deposition (ALD): From precursors to thin film structures," *Thin Solid Films* 409(1), 138-146. DOI: 10.1016/S0040-6090(02)00117-7

Li, Y., Chen, L., Wooding, J. P., Zhang, F., Lively, R. P., Ramprasad, R., and Losego, M. D. (2020). "Controlling wettability, wet strength, and fluid transport selectivity of nanopaper with atomic layer deposited (ALD) sub-nanometer metal oxide coatings," *Nanoscale Adv.* 2(1), 356-367. DOI: 10.1039/c9na00417c

Lu, J., Li, Y., Song, W., Losego, M. D., Monikandan, R., Jacob, K. I., and Xiao, R. (2020). "Atomic layer deposition onto thermoplastic polymeric nanofibrous aerogel templates for tailored surface properties," *ACS Nano* 14(7), 7999-8011. DOI: 10.1021/acsnano.9b09497

Mangolini, F., McClimon, J. B., Rose, F., and Carpick, R. W. (2014). "Accounting for nanometer-thick adventitious carbon contamination in X-ray absorption spectra of carbon-based materials," *Anal. Chem.* 86(24), 12258-12265. DOI: 10.1021/ac503409c.

Mirvakili, M. N., Van Bui, H., Van Ommen, J. R., Hatzikiriakos, S. G., and Englezos, P. (2016). "Enhanced barrier performance of engineered paper by atomic layer deposited Al_2O_3 thin films," *ACS Appl. Mater. Interfaces* 8(21), 13590-13600. DOI: 10.1021/acsami.6b02292

Nair, S. S., Zhu, J., Deng, Y., and Ragauskas, A. J. (2014). "High performance green barriers based on nanocellulose," *Sustain. Chem. Process.* 2(1), 1-7. DOI: 10.1186/s40508-014-0023-0

Obuchovsky, S., Frankenstein, H., Vinokur, J., Hailey, A. K., Loo, Y. L., and Frey, G. L. (2016). "Mechanism of metal oxide deposition from atomic layer deposition inside nonreactive polymer matrices: Effects of polymer crystallinity and temperature," *Chem. Mater.* 28(8), 2668-2676. DOI: 10.1021/acs.chemmater.6b00159

Peng, Q., Sun, X. Y., Spagnola, J. C., Hyde, G. K., Spontak, R. J., and Parsons, G. N. (2007). "Atomic layer deposition on electrospun polymer fibers as a direct route to Al_2O_3 microtubes with precise wall thickness control," *Nano Lett.* 7(3), 719-722. DOI: 10.1021/nl062948i

Puurunen, R. L. (2005). "Surface chemistry of atomic layer deposition: A case study for the trimethylaluminum/water process," *J. Appl. Phys.* 97, 121301-121301-52. DOI: 10.1063/1.1940727

Ritala, M., Leskelä, M., Nykänen, E., Soininen, P., and Niinistö, L. (1993). "Growth of titanium dioxide thin films by atomic layer epitaxy," *Thin Solid Films* 225(1–2), 288-295. DOI: 10.1016/0040-6090(93)90172-L

Sammelselg, V., Rosental, A., Tarre, A., Niinistö, L., Heiskanen, K., Ilmonen, K., Johansson, L. S., and Uustare, T. (1998). "TiO_2 thin films by atomic layer deposition: A case of uneven growth at low temperature," *Appl. Surf. Sci.* 134(1–4), 78-86. DOI: 10.1016/S0169-4332(98)00224-4

Short, A. E., Pamidi, S. V., Bloomberg, Z. E., Li, Y., and Losego, M. D. (2019). "Atomic layer deposition (ALD) of subnanometer inorganic layers on natural cotton to enhance oil sorption performance in marine environments," *J. Mater. Res.* 34(4), 563-570. DOI: 10.1557/jmr.2018.441

Spagnola, J. C., Gong, B., Arvidson, S. A., Jur, J. S., Khan, S. A., and Parsons, G. N. (2010). "Surface and sub-surface reactions during low temperature aluminium oxide atomic layer deposition on fiber-forming polymers," *J. Mater. Chem.* 20, 4213-4222. DOI: 10.1039/c0jm00355g

Spence, K. L., Venditti, R. A., Rojas, O. J., Habibi, Y., and Pawlak, J. J. (2010). "The effect of chemical composition on microfibrillar cellulose films from wood pulps: Water interactions and physical properties for packaging applications," *Cellulose* 17(4), 835-848. DOI: 10.1007/s10570-010-9424-8

The Ellen MacArthur Foundation (2017). "The New Plastics Economy: Catalysing Action," *Ellen MacArthur Found.* https://ellenmacarthurfoundation.org/the-new-plastics-economy-catalysing-action.

Vähä-Nissi, M., Sievänen, J., Salo, E., Heikkilä, P., Kenttä, E., Johansson, L. S., Koskinen, J. T., and Harlin, A. (2014). "Atomic and molecular layer deposition for surface modification," *J. Solid State Chem.* 214, 7-11. DOI: 10.1016/j.jssc.2013.11.040

Vähä-Nissi, M., Sundberg, P., Kauppi, E., Hirvikorpi, T., Sievänen, J., Sood, A., Karppinen, M., and Harlin, A. (2012). "Barrier properties of Al_2O_3 and alucone coatings and nanolaminates on flexible biopolymer films," *Thin Solid Films* 520(22), 6780-6785. Elsevier B.V. DOI: 10.1016/j.tsf.2012.07.025

Viitala, J., Lappalainen, T., and Järvinen, M. (2020). "Sodium dodecyl sulphate (SDS) residue analysis of foam-formed cellulose-based products," *Nord. Pulp Pap. Res. J.* 35(2), 261-271. DOI: 10.1515/npprj-2019-0058

Wilson, C. A., Grubbs, R. K., and George, S. M. (2005). "Nucleation and growth during Al2O3 atomic layer deposition on polymers," *Chem. Mater.* 17(23), 5625-5634. DOI: 10.1021/cm050704d

Wooding, J. P., Li, Y., Kalaitzidou, K., and Losego, M. D. (2020). "Engineering the interfacial chemistry and mechanical properties of cellulose-reinforced epoxy composites using atomic layer deposition (ALD)," *Cellulose* 27(11), 6275-6285. DOI: 10.1007/s10570-020-03188-5

Xu, Y., and Musgrave, C. B. (2004). "A DFT study of the Al_2O_3 atomic layer deposition on SAMs: Effect of SAM termination," *Chem. Mater.* (16), 639-645. DOI: 10.1021/cm035009p

Zhang, L., Patil, A.J., Li, L., Schierhorn, A., Mann, S., Gösele, U., and Knez, M. (2009). "Chemical infiltration during atomic layer deposition: Metalation of porphyrins as model substrates," *Angew. Chemie - Int. Ed.* 48(27), 4982-4985. DOI: 10.1002/anie.200900426

Article submitted: August 25, 2023; Peer review completed: September 9, 2023; Revised version received and accepted: September 22, 2023; Published: October 5, 2023.
DOI: 10.15376/biores.18.4.7923-7942